Location and environmental eld characteristics of non-Mountain Wave Turbulence around a Meiyu-Baiu front

V13 - 25ARAM

Soshi Ito[1]、Yoshiaki MIyamoto[1,2]
1:Keio University、2:RIKEN Cneter for Computational Science
Name:Soshi Ito
e-mail:soshiitoh@keio.jp

INTRODUCTION and OBJECTIVES

Aviation turbulence is a major factor in weather-related aviation accidents [Gultepe et al., 2019]. It is classified into clear air turbulence (CAT), mountain wave turbulence (MWT), and convectively induced turbulence (CIT), depending on the source [Kim et al., 2018]. CAT occurs in clear air around the jet stream, at the tropopause, and at the upper front [Venkatesh and Mathew, 2013; Sharman and Lane, 2016]. The MWT is the one in which topography is a factor. CIT occurs in and out of clouds with convection, while near-cloud turbulence (NCT) occurs near clouds [Lane et al., 2012]. There have been several proposed mechanisms for the formation of NCT [e.g., Lane and Sharman, 2008; Sharman and Lane, 2016; Kim et al., 2019], but the mechanism varies depending on the cloud form and occurrence [Sharman and Trier, 2019].

We have analyzed the average environmental field during the occurrence of clear air turbulence above 400 hPa over Japan [Ito et al., under review]. The results suggest that in June, reported turbulence is often located north of the point of the Baiu front. Few studies have clarified the relationship between the Baiu front and turbulence, and there are many unanswered questions, such as the extent to which the Baiu front contributes to the generation of turbulence.

This study aims to characterize the number of reports and the environmental field at the time of the encounter by distance from the Baiu front for CAT and CIT. By analyzing the environmental fields at different distances, it is possible to show the extent to which the Baiu front is a source of turbulence.

ANALYSIS METHOD

- **Data Used**

Data 1: Pilot Report (PIREP)

PIREP is notified when a pilot encounters a weather phenomenon while cruising. The coordinates, altitude, strength, and date and time of the turbulence encounter are available.

Data 2: JMA-Meso Analysis (MANAL)

MANAL is reanalysis data. The area around Japan is divided vertically into 15 layers up to 50 hPa, with a horizontal resolution of 5 km and a temporal resolution of 3 h. MANAL includes zonal wind, meridional wind, temperature, and relative humidity.

Data 3: Collaborative Actions for Renovation of Air Traffic Systems (CARATS) open data

CARATS open data on flight paths around Japan is provided by the Ministry of Land, Infrastructure, Transport and Tourism (MLIT) of Japan. It includes altitude, latitude, and longitude at approximately 10-second intervals.

The analysis period was 2010-2017 for PIREP and MANAL and May 2012 for CARATS open data. We focused on the moderate-intensity cases of CAT and CIT above 400 hPa.

- **Analysis Method**

For the analysis period May-July, we identified the Baiu front at the time of turbulence, referring to Tomita et al. (2011) and Li et al. (2018). We calculated the shortest distance from the Baiu front for each turbulence case. Using MANAL, we created meteorological field datasets for each turbulence case at the time and altitude of occurrence. These datasets were used to calculate multiple turbulence indices. Probability density functions were computed for each group. Similar calculations were performed for winter CAT cases. Additionally, we calculated the average environmental field for each group over a 1600 km square area centered on the turbulence encounter point.

Horizontal Distribution of Turbulence

Figure 1 shows that encounters were more frequent on the southern side towards the west. Additionally, encounters were more frequent in the region between 36-40°N and 142-146°E. However, this suggests that encounters can occur anywhere along flight routes.

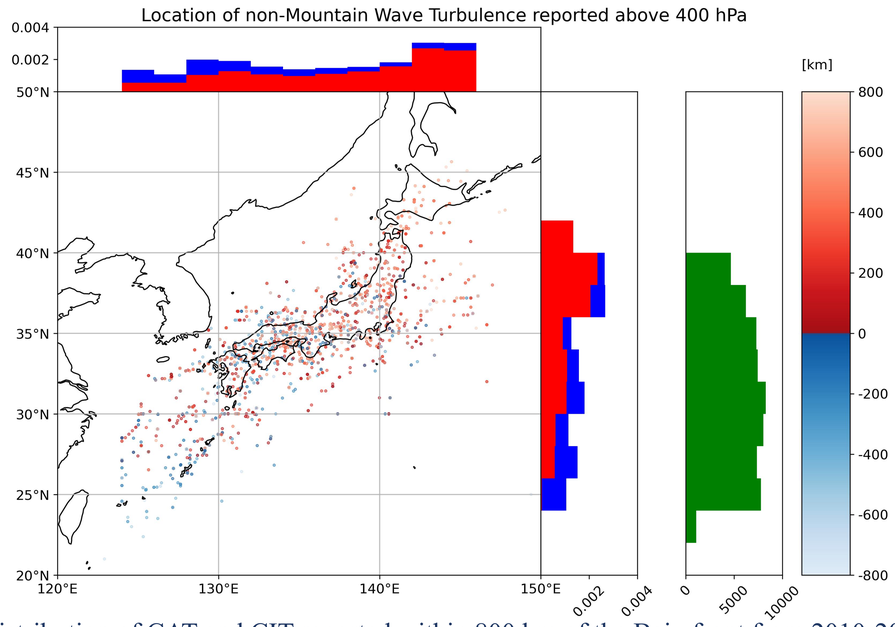


Fig. 1: Spatial distribution of CAT and CIT reported within 800 km of the Baiu front from 2010-2017 in May-July. Dots indicate the north and south of the Baiu front, respectively. The histograms at the top and right show the number divided by the number of flights, by longitude and latitude, respectively. Red and blue indicate cases reported north and south of the Baiu front, respectively. The green histogram shows the average latitude for each extracted Meiyu-Baiu front. The width of the histogram bins is 2 degrees.

Figure 2 shows that there were more encounters on the northern side than on the southern side. The highest number of encounters occurred in the region 300-400 km north of the Baiu front, with encounter frequency decreasing with distance from this zone.

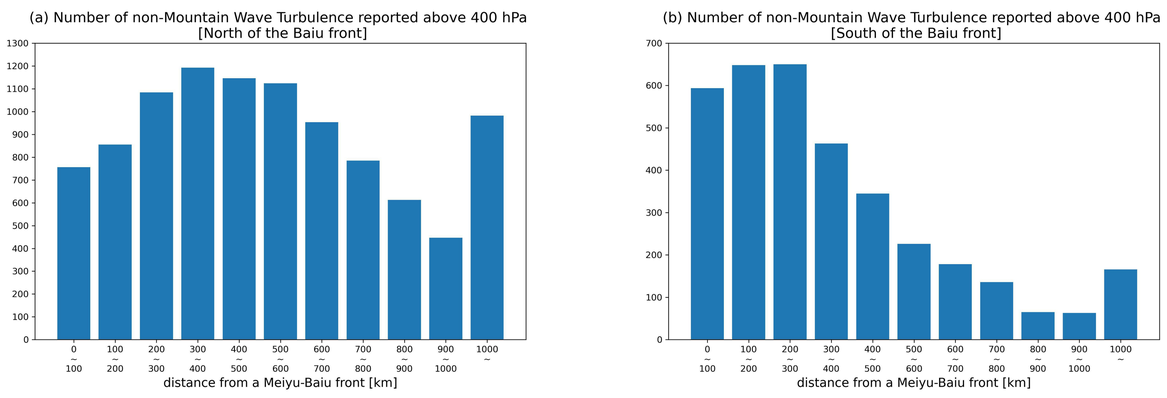
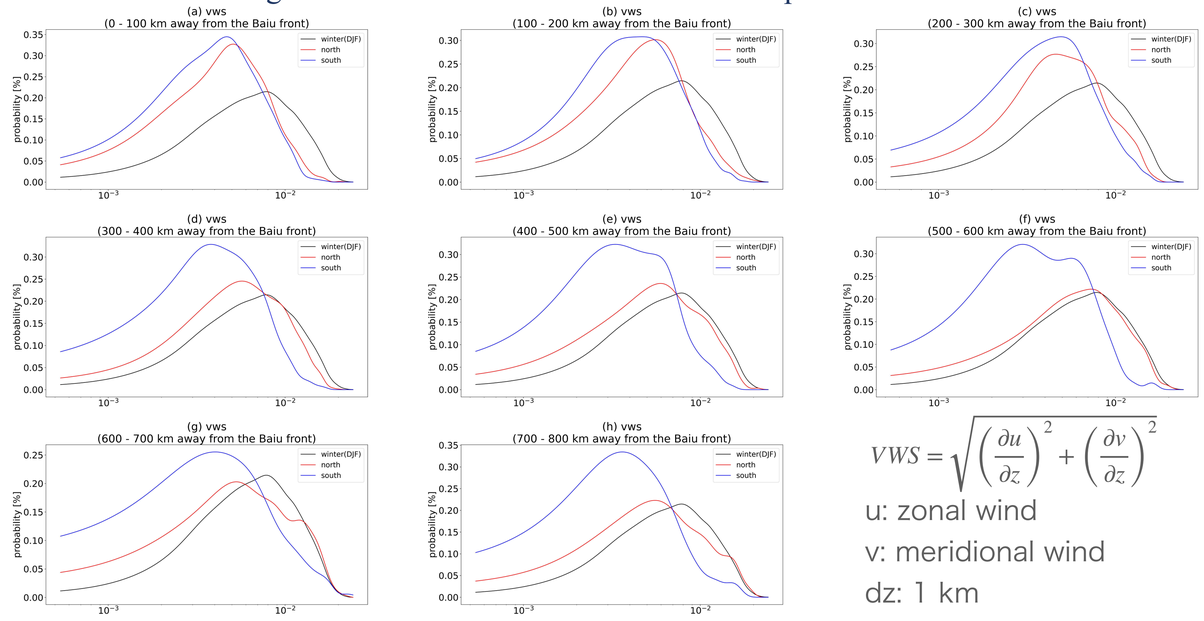


Fig. 2: Histograms of CAT and CIT of moderate intensity reported above 400 hPa from 2010-2017 in May-July by distance from the Baiu front. Those reported (a) north and (b) south of the Baiu front are shown, respectively. The vertical axis shows the number and the horizontal axis shows the distance from the Baiu front.

Probability Density Function of Vertical Wind Shear

Figure 3 shows that the region 300-800 km north of the Baiu front had a similar distribution, and the region 500-600 km away had a distribution almost identical to the winter distribution. Other regions had peak values weaker than the winter distribution, and the 0-300 km northern region and 0-800 km southern region exhibited different distributions compared to the winter.



$$VWS = \sqrt{\left(\frac{\partial u}{\partial z}\right)^2 + \left(\frac{\partial v}{\partial z}\right)^2}$$

u: zonal wind
v: meridional wind
dz: 1 km

Fig. 3: This shows the probability density functions (PDFs) of VWS at occurrence points for CAT and CIT events that occurred from May to July 2010-2017 and CAT events that occurred in December, January, and February (winter). Winter cases are shown in black, cases that occurred north of the Baiu front are shown in red, and cases that occurred south of the Baiu front are shown in blue. The vertical axis indicates the PDF, and the horizontal axis indicates the log scale for the size of the VWS, respectively. (a)-(h) shows the classification of the distance from the Baiu front by 100 km.

The Average Horizontal Distribution

Figure 4 shows that the VWS was strong in the region 300-800 km north of the Baiu front. Figure 5 shows that the VWS was weak in the region 0-500 km south of the Baiu front.

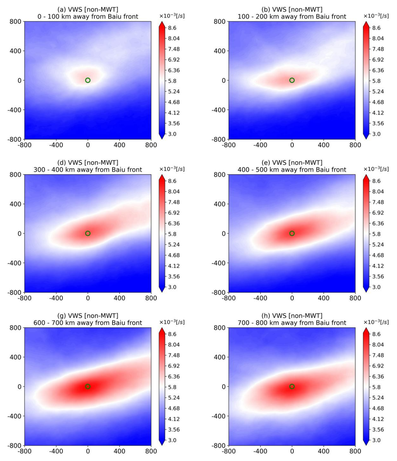


Fig. 4: The composited horizontal distribution of VWS in a 1600 km square area centered on the point where turbulence was reported at altitudes above 400 hPa for moderate CAT and CIT cases that occurred north of the Baiu front. The horizontal and vertical axes indicate the distance from the point of encounter. The green circle stands for the location of reported turbulence. (a)-(h) shows the classification of the distance from the Baiu front by 100 km.

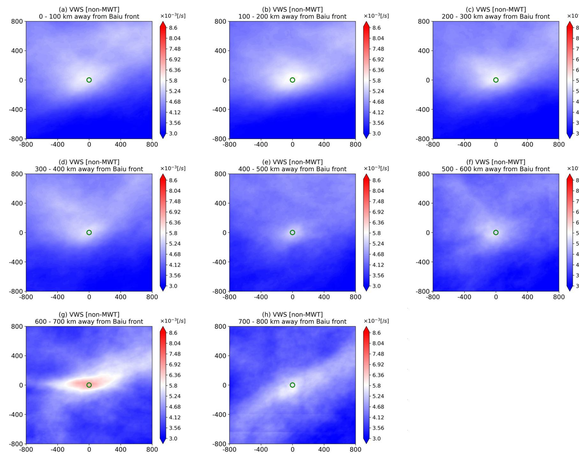
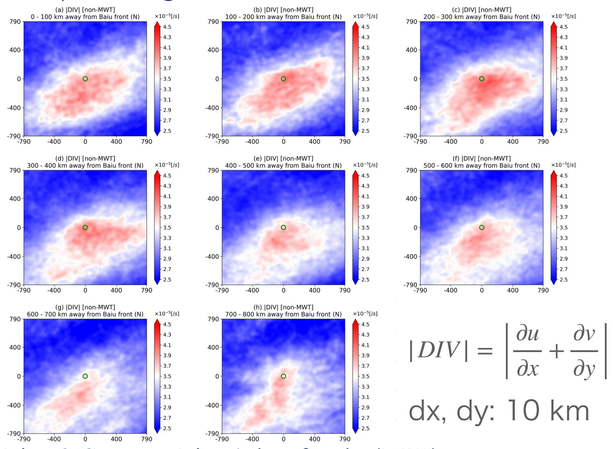


Fig. 5: Same as Fig. 4, but turbulence that occurred south of the Baiu front.

Figures 6 and 7 show that the region of 0-500 km to the south of the Baiu front had the strongest |DIV|. The region of 0-400 km to the north was the strongest |DIV| among the northern regions.



$$|DIV| = \left|\frac{\partial u}{\partial x} + \frac{\partial v}{\partial y}\right|$$

dx, dy: 10 km

Fig. 6: Same as Fig. 4, but for the |DIV|.

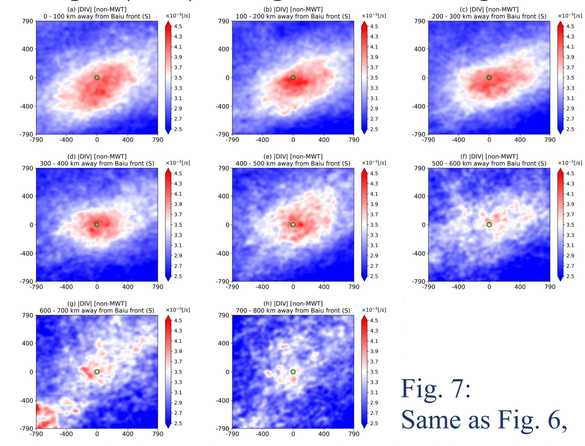


Fig. 7: Same as Fig. 6, but turbulence that occurred south of the Baiu front.

DISCUSSION and CONCLUSION

North, 400-800 km	‣ The VWS was strong, and the PDF distribution at 500-600 km was similar to that in winter. ‣ Deformation and The horizontal gradient of temperature were also strong (not shown in the figure). ‣ The strengthening of deformation enhances VWS, making it more likely for turbulence to occur. ‣ Upper-level winds tend to be enhanced along the northern edge of the Baiu front [Akiyama, 1973].
South, 0-500 km	‣ The VWS was weak, and the IDIVI was strong. ‣ There was a moist strong convergence field in the lower level (not shown in the figure). ‣ The strong convection in the lower layer extends up to the altitude of the turbulence generation, which suggests that convection or convective gravity waves can easily generate turbulence in this environment.

We have extracted the Baiu front and analyzed the probability density function (PDF) of turbulence indices and the environmental conditions at different distances from the Baiu front using historical turbulence occurrence data. The favorable environmental conditions for turbulence were found to be different between the northern region, located 400-800 km away, and the southern region, situated 0-500 km away from the Baiu front. In the future, we plan to conduct case studies in the region 0-500 km south of the target area to clarify how the strong convection associated with the Baiu front influences the generation of turbulence.

This work is supported by JST SPRING, Grant Number JPMJSP2123.

• Akiyama, T. 1973: Pap.Met.Geophy, 24, 157–188.
• Gultepe, I. et al. 2019: Pure Appl. Geophys., 176, 1869–1921.
• Kim, J.-H., et al. 2018: Bulletin of the American Meteorological Society, 99, 2295–2311.
• Kim, S.-H., et al. 2019: Journal of Applied Meteorology and Climatology, 58, 1725–1750.
• Lane, T. P., and R. D. Sharman. 2008: Journal of Applied Meteorology and Climatology, 47, 2777–2796.
• Lane, T. P., et al. 2012: Bulletin of the American Meteorological Society, 93, 499–515.
• Li, Y., et al. 2018: Clim Dyn, 51, 1659–1670.
• Sharman, R., and T. Lane Eds. 2016: Springer International Publishing.
• Sharman, R. D., and S. B. Trier. 2019: Pure Appl. Geophys., 176, 1923–1958.
• Tomita, T., et al. 2011: Journal of the Meteorological Society of Japan, 89, 517–537.
• Venkatesh, T. N., and J. Mathew. 2013: Sadhana, 38, 707–722.